Supporting Information for "Methane occurrence and quantification in a very shallow water environment: a multidisciplinary approach"

G. M. Ferrante *, F. Donda[1], V. Volpi[1], U. Tinivella[1]and M. Adelinet[2]

[1]Istituto Nazionale di Oceanografia e di Geofisica Sperimentale — OGS, Trieste, Italy

[2]IFP Energies nouvelles, Rueil-Malmaison Cedex, France

Contents of this file

1. Text S1 to S4
2. Figures S1 to S3

Introduction

This supplementary information contains additional details on the analysis and results of the gas quantification procedure explained in the main text. In particular, we include (i) the flow diagrams summarizing the processing applied to the seismic data; (ii) the P-wave velocity and porosity sections resulted from the seismic-well logs correlation; (iii)

Corresponding author: G. M. Ferrante, 19 rue érard, Paris, 75012, France. (matildeferrante@hotmail.com)

*19 rue érard, 75012, Paris

the estimated saturation exponent n section required for the final gas quantification and (iv) the inherent assumptions and uncertainties of the methodology.

Text S1.

We report the flow charts for the A) imaging and B) true-amplitude seismic processing. The sequence A) includes: noise removal (random noise, refractions, out-of-plane reflections and reverberations), through manual editing and the application of bandpass filters in time-space, frequency-wavenumber and tau-p domain; multiple attenuation with the application of predictive deconvolution before and post stack; pre-stack time Kirchhoff migration. The flow of the sequence B) is mainly aimed at attenuating multiple events without affecting the original amplitude information, which should be preserved for quantifying the gas content. For this reason, migration and deconvolution algorithms are banned. Instead, the amplitude-preserving surface-related multiple elimination technique for multiple attenuation is used.

Text S2.

We report P-wave velocity and porosity results from the seismic-well logs multi-attributes correlation. Starting from the well log information, the spatial distribution of petrophysical properties has been imaged along the STENAP 08 and GANDI 09 (Figure S2) seismic lines, as described in the main text. Log data are the available sonic and resistivity profiles and the calculated EMT-based porosity pseudo-log. The seismic data used are the amplitude preserving stack section for the STENAP 08 seismic line and a time-migrated stack section for the GANDI 09 seismic line. In fact, it was not possible to successfully correlate logs and the amplitude preserving stack of the GANDI 09 seismic

line. This is because of the strong amplitude variations and the diffuse blanking. Neither velocity nor porosity sections show any significant gas-related anomaly.

Text S3.

We report the saturation exponent n sections for the STENAP 08 and the GANDI 09 (Figure S3) seismic lines, estimated as explained in the main text. Note that, due to the lack of constraints, in the case of the GANDI 09 seismic line, we decided to manually assign n values to the main geological units. These values have been calibrated on the STENAP 08 seismic line, at the crossing point with the GANDI 09.

Text S4.

Although both the inversion procedure used to estimate porosity and the log-seismic correlation have been validated with a very stringent control of uncertainty (details in the text), the method presented in this work still includes a certain number of assumptions. These encompass: i) the density values assigned to the recognized lithostratigraphic facies; ii) the elastic moduli of the rocks and fluid mixture; iii) the assumptions made on pore structure and distribution; iv) the hypothesis of pore total saturation. Moreover, our results are obviously affected by the uncertainty derived from the lithostratigraphic interpretation, done by an operator as described in the text, and cannot be quantified. Lastly, a further source of error lies in the procedure used to estimate the saturation exponent n in the final gas content quantification through Archie's Law. In this regard, we tested several n values $\in (0, 10)$ in Eq.4 and find that the final results have very little sensitivity to this parameter.

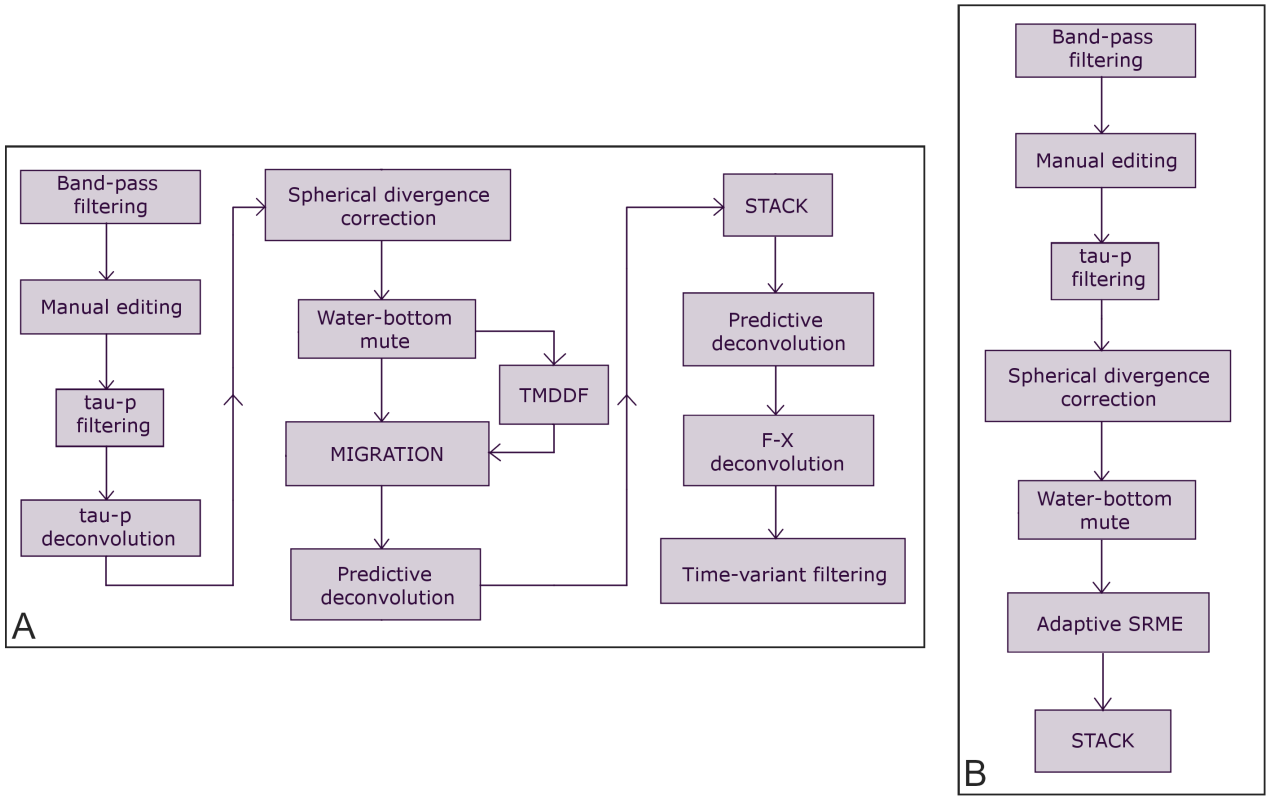

Figure S1. Flow charts for A) the imaging and B) the true-amplitude seismic processing.

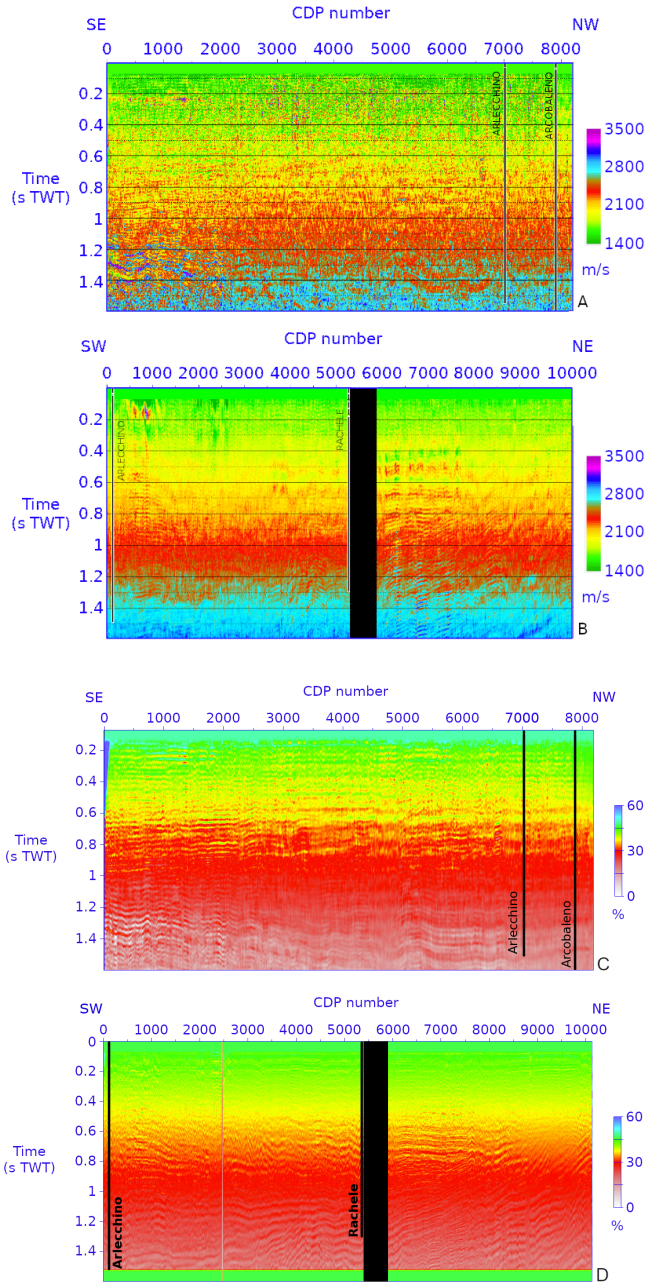

Figure S2. Velocity sections and porosity sections for the STENAP 08 (A and C) and the GANDI 09 (B and D) lines, resulted from the seismic-well logs multi-attribute correlation. Well locations are shown. Black box indicates a zone of no coverage.

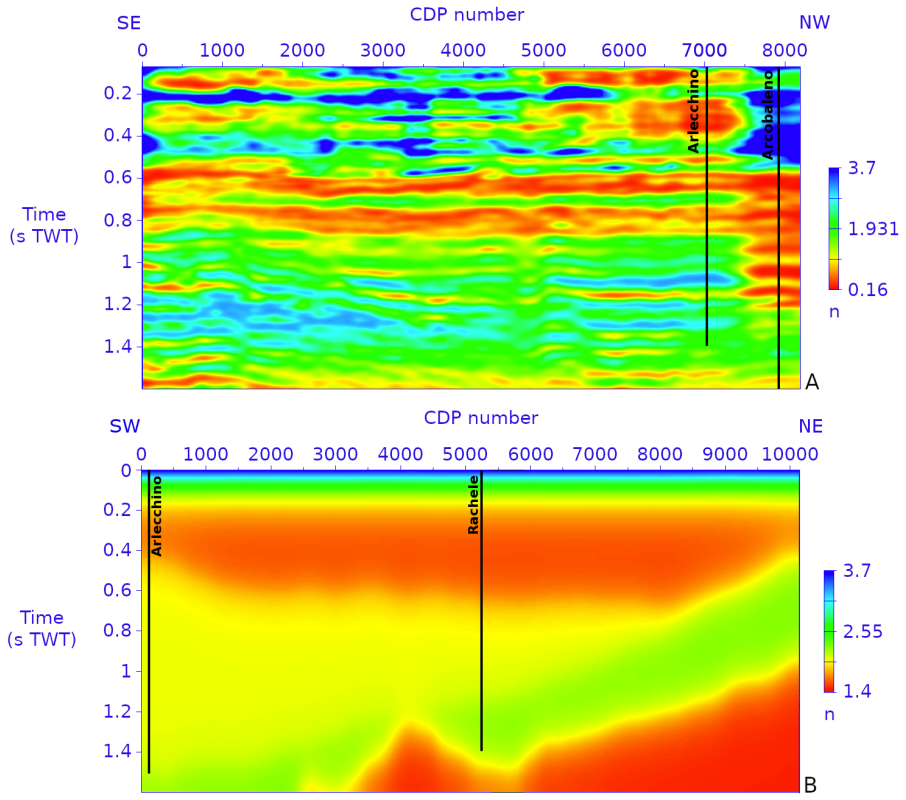

Figure S3. A) STENAP 08 and B) GANDI 09 saturation exponent n sections. Well locations are shown.